

Vorlanite, (CaU⁶⁺)O₄, from Jabel Harmun, Palestinian Autonomy, Israel

EVGENY V. GALUSKIN,^{1*} JOACHIM KUSZ,² THOMAS ARMBRUSTER,³

IRINA O. GALUSKINA,¹ KATARZYNA MARZEC⁴, YEVGENY VAPNIK⁵, MIKHAIL MURASHKO⁶

¹Faculty of Earth Sciences, Department of Geochemistry, Mineralogy and Petrography, University
of Silesia, Będzińska 60, 41-200 Sosnowiec, Poland

*E-mail: evgeny.galuskin@us.edu.pl

²Institute of Physics, University of Silesia, Uniwersytecka 4, 40-007 Katowice, Poland

³Mineralogical Crystallography, Institute of Geological Sciences, University of Bern,
Freiestrasse 3, CH-3012 Bern, Switzerland

⁴Jagiellonian Centre for Experimental Therapeutics, Bobrzyńskiego 14, 30-348 Cracow, Poland

⁵Department of Geological and Environmental Sciences, Ben-Gurion University of the Negev,
POB 653, Beer-Sheva 84105, Israel

⁶Systematic Mineralogy, 44, 11th line V.O, apt. 76, Saint-Petersburg 199178, Russia

28

29 **ABSTRACT**

30 Vorlanite ($\text{CaU}^{6+}\text{O}_4$) ($Fm\bar{3}m$, $a = 5.3647(9) \text{ \AA}$, $V = 154.40(4) \text{ \AA}^3$, $Z = 2$) was found in larnite
31 pyrometamorphic rocks of the Hatrurim formation at the Jabel Harmun locality, Judean Desert,
32 Palestinian Autonomy. Black vorlanite crystals from these larnite rocks are dark-grey with greenish
33 hue in transmitted light. This color in transmitted light is in contrast to dark-red vorlanite ($Fm\bar{3}m$,
34 $a = 5.3813(2) \text{ \AA}$, $V = 155.834(10) \text{ \AA}^3$, $Z = 2$) from the type locality Upper Chegem caldera, Northern
35 Caucasus. Heating above 750°C of dark-grey vorlanite from the Jabel Harmun, as well as dark-red
36 vorlanite from Caucasus, led to formation of yellow trigonal uranate CaUO_4 . The unusual color of
37 vorlanite from Jabel Harmun is assumed to be related to small impurities of tetravalent uranium.

38

39 **Keywords:** vorlanite, structure, Raman spectroscopy, lakargiite, Hatrurim formation, Jabel
40 Harmun, Judean Desert.

41

42

43

44

45

46

47

48

49

50

51

52

53

54

55 INTRODUCTION

56 Vorlanite, $(\text{CaU}^{6+})\text{O}_4$, a mineral with radiation-induced disordered structure of the fluorite
57 type, was originally discovered in altered xenoliths within ignimbrites of the Upper Chegem
58 caldera, Vorlan Mountain, Northern Caucasus, Kabardino-Balkaria (Galuskin et al. 2009, 2011).

59 Vorlanite occurs also as rare accessory mineral in larnite and spurrite pyrometamorphic
60 rocks of the Hatrurim formation. Rocks of the Hatrurim formation are widely distributed in the
61 region of the Dead Sea on the territory of Israel, Palestinian Autonomy and Jordan (Picard 1931;
62 Kolodny and Gross 1974; Burg et al. 1991, 1999). We detected numerous black platy vorlanite
63 crystals in larnite pyrometamorphic rocks from the Jabel Harmun locality, Judean Desert,
64 Palestinian Autonomy, Israel. The remarkable property of vorlanite from the Jabel Harmun in
65 contrast to Caucasian vorlanite is its dark-grey color with greenish hue in transmitted light (Fig. 1).

66 Vorlanite, $(\text{CaU}^{6+})\text{O}_4$, from Caucasus ($Fm\bar{3}m$, $a = 5.3813(2) \text{ \AA}$) formed out of the trigonal
67 calcium uranate CaUO_4 ($R\bar{3}m$, $a = 3.878 \text{ \AA}$, $b = 17.564 \text{ \AA}$) where α -decay events of uranium
68 caused disordering of Ca and U associated with randomly oriented uranyl-bonds (Galuskin et al.
69 2012). Vorlanite experienced 0.56 displacements per atom (dpa) during α -decay events (Galuskin et
70 al. 2011). Caucasian vorlanite is black in hand specimens but dark-red in transmitted light, which is
71 highly surprising for minerals containing hexavalent uranium. In addition, the platy crystals
72 inherited the morphology of “protovorlanite” – a trigonal uranate. Above 750°C dark-red disordered
73 vorlanite transformed irreversibly to bright-yellow, ordered, trigonal uranate (Galuskin et al. 2012).

74 Most recently vorlanite was also described as tiny inclusions in uranium-bearing opals from
75 Sierra Pieña Blanca, Mexico (Othmane et al. 2013). It was assumed that these nanocrystals formed
76 under oxidizing conditions below 50°C. However, this finding requires additional investigations
77 because composition and structure of this unusual mineral may also be interpreted as Ca-rich
78 uraninite. In addition, the nanocrystals did not form by radiation-induced transformation from the

79 trigonal precursor “protovorlanite” CaUO_4 with ordered $[\text{UO}_2]^{2+}$ groups (Galuskin et al. 2011,
80 2012).

81 In this paper we present results of structure, composition and Raman spectroscopy
82 experiments aiming at recovery of the primary structure of dark-grey vorlanite from the Judean
83 Desert.

84

85 **Methods of investigations**

86 Crystal morphology and chemical composition of vorlanite and associated minerals were
87 examined using optical microscopes, analytical electron scanning microscope Philips XL30
88 ESEM/EDAX (Faculty of Earth Sciences, University of Silesia, Poland) and electron microprobe
89 CAMECA SX100 (Institute of Geochemistry, Mineralogy and Petrology, University of Warsaw,
90 Poland). Electron-microprobe analyses of vorlanite were performed at 15 kV and 40–50 nA using
91 the following lines and standards: $\text{UM}\beta$ for Caucasian vorlanite, $\text{CaK}\alpha$ for wollastonite and
92 diopside; $\text{FeK}\alpha$ for hematite.

93 The Raman spectra of vorlanite were recorded using a WITec confocal CRM alpha 300
94 Raman microscope (Jagiellonian Centre for Experimental Therapeutics, Cracow, Poland) equipped
95 with an air-cooled solid-state laser operating at 488 nm and a CCD detector which was cooled to -
96 82°C. The laser was coupled to the microscope via a single-mode optical fibre with a diameter of 50
97 μm . A dry Olympus MPLAN (1006/0.90NA) objective was used. The scattered radiation was
98 focused onto a multi-mode fibre (50 μm diameter) and monochromator. The power of the laser at
99 the sample position was 44 mW for measurement and 100-120 mW for heating and crater
100 production. 150 scans with integration times of 0.3-0.5 s and a resolution of 3 cm^{-1} were collected
101 and averaged. The monochromator of spectrometer is calibrated using the Raman scattering line
102 produced by a silicon plate (520.7 cm^{-1}).

103 Single-crystal X-ray studies of vorlanite from Israel were carried out using a SuperNova
104 Dual diffractometer with a mirror monochromator ($\text{MoK}\alpha_1 = 0.71073\text{ \AA}$) and Atlas CCD detector

105 (Agilent Technologies) at the Institute of Physics, University of Silesia, Poland. Experimental
106 details are summarized in Table 2. The structure was solved by direct methods, with subsequent
107 analyses of difference-Fourier maps, and refined with neutral atom scattering factors using
108 SHELX97 (Sheldrick 2008).

109

110 **RESULTS OF INVESTIGATIONS OF DARK-GREY VORLANITE AND DISCUSSION**

111 Crystals of dark-grey vorlanite were found in dark-brown larnite pebbles hosted in rock
112 known as pseudoconglomerate. Larnite rocks have been originally formed by pyrogenic
113 metamorphism due to caustobiolith combustion at temperatures above 1000°C (Kolodny and Gross
114 1974; Sokol et al. 2007, 2010). Their pebble-like shape can be explained by low-temperature
115 hydrothermal processes with subsequent weathering of larnite rocks (Gross 1977). Larnite β -
116 Ca_2SiO_4 , ye'elimite $\text{Ca}_4\text{Al}_6\text{O}_{12}(\text{SO}_4)$, fluorine analogs of the mayenite-kyuygenite series
117 $\text{Ca}_{12}\text{Al}_{14}\text{O}_{32}\text{F}_2$ – $\text{Ca}_{12}\text{Al}_{14}\text{O}_{32}[\text{F}_2(\text{H}_2\text{O})_4]$, fluorellestadite $\text{Ca}_5(\text{SiO}_4)_{1.5}(\text{SO}_4)_{1.5}\text{F}$, ternesite
118 $\text{Ca}_5(\text{SiO}_4)_2(\text{SO}_4)$, brownmillerite $\text{Ca}_2\text{Fe}^{3+}\text{AlO}_5$ –srebrodolskite $\text{Ca}_2\text{Fe}^{3+}\text{Fe}^{3+}\text{O}_5$, shulamitite
119 $\text{Ca}_3\text{Ti}^{4+}\text{Fe}^{3+}\text{AlO}_8$ – Fe^{3+} -analog of shulamitite $\text{Ca}_3\text{Ti}^{4+}\text{Fe}^{3+}\text{Fe}^{3+}\text{O}_8$ are the main minerals of these
120 pebbles. Kyuygenite with the end-member formula $\text{Ca}_{12}\text{Al}_{14}\text{O}_{32}[\text{Cl}_2(\text{H}_2\text{O})_4]$ was recently discovered
121 in high-temperature skarns of the Upper Chegem caldera in Caucasus (Galuskin et al. 2013a).
122 Shulamitite detected in pyrometamorphic rocks of the Hatrurim Basin, Negev Desert (the Hatrurim
123 formation) was recently approved by IMA-CNMNC (Sharygin et al. 2013). Rare oldhamite CaS ,
124 periclase MgO , magnesioferrite MgFe_2O_4 , baryte BaSO_4 , and the recently discovered minerals
125 nabimusaitite $\text{KCa}_{12}(\text{SiO}_4)_4(\text{SO}_4)_2\text{O}_2\text{F}$ (Galuskin et al. 2013b) and harmunitite CaFe_2O_4 (Galuskina et
126 al. 2013) and also undiagnosed K-sulfides and potentially new minerals Ca_3UO_6 and CaCu_2S_2 are
127 noted. Vorlanite forms typical poikilitic crystals (Fig. 1), related to its crystallization after larnite,
128 mayenite and ye'elimite.

129 Composition and structure of dark-grey vorlanite from Jabel Harmun are analogous to
130 composition and structure of dark-red vorlanite from Caucasus (Table 1-4, Galuskin et al. 2011).
131 The chemical composition of vorlanite corresponds to stoichiometric CaUO_4 . Site occupancies

5

132 determined by using single crystal X-ray diffraction data are consistent with a fully occupied O site,
133 with a Ca/U ratio = 1 confirming that practically all uranium has valence 6+ (Table 3). This
134 conclusion was proven for vorlanite from Caucasus by XPS investigations (Galuskin et al. 2011).

135 Raman spectra of dark-red vorlanite from Caucasus and dark-grey vorlanite from Israel are
136 similar, the one strong broad band centered near 683 cm^{-1} is present in both spectra (Fig. 2, spectra
137 1 and 2). A Raman spectroscopic local heating experiment on dark-grey vorlanite from Jabel
138 Harmun with a blue laser (488 nm) above 750°C produced in close vicinity to the crater trigonal
139 uranate CaUO_4 . This newly produced phase is indicated by appearance of a yellow ring around the
140 crater (Fig. 1C). Heating of vorlanite from both localities above 750°C led to the same result –
141 ordered trigonal calcium uranate forms after vorlanite. The Raman spectra of the heat produced
142 phases correspond exactly to the Raman spectrum of the known synthetic phase (Liegeois-
143 Duyckaerts 1977; Fig. 2, spectra 1* and 2*).

144 The accepted structural model for vorlanite suggests that U and Ca randomly occupy a
145 single eightfold-coordinated site with mean metal (M) to oxygen (O) distances M-O of $8 \times 2.33\text{ \AA}$.
146 However, Raman investigations on vorlanite indicate that there are also short U-O bonds $< 2\text{ \AA}$
147 characteristic of the uranyl group $(\text{UO}_2)^{2+}$ (Galuskin et al. 2011), i.e. the true local U-coordination is
148 6+2. It was assumed that in the real structure of vorlanite not only the positions of the cations Ca
149 and U are disordered over a single site, but there is also “uranyl disorder”, i.e. O-U-O uranyl bonds
150 are randomly aligned parallel to one of the four symmetry-equivalent cube diagonals (Galuskin et
151 al. 2011).

152 A basic difference between vorlanite from Jabel Harmun and Caucasian vorlanite is the
153 dark-grey color with greenish hue in transmitted light of the former vorlanite. This color could
154 indicate that not all uranium is hexavalent. Color change of synthetic trigonal uranate CaUO_4 from
155 yellow to dark-green was observed on heating above 1100°C , when the disordered phase with
156 fluorite-type structure formed and the composition corresponded to $\text{CaU}_2\text{O}_{5+y}$ (Terra et al. 2008).
157 Takagawa et al. (1977) synthesized nonstoichiometric dark green or dark grey uranate $\text{SrUO}_{3.18-3.20}$

158 at 1000°C in hydrogen atmosphere. The color of these uranates changed to red when exposed to air
159 after three months and the corresponding X-ray diffraction pattern indicated that structure and cell
160 parameters of the red phase were in agreement with rhombohedral α -SrUO₄.

161 Tetraivalent uranium may substitute in vorlanite according to the known isomorphic scheme
162 for uraninite: $\text{CaU}^{6+} \rightarrow 2\text{U}^{4+}$ (Janeczek and Ewing 1992). In addition, precursor of vorlanite
163 corresponds to the O-deficient synthetic phase CaUO_{4-x} with $x < 0.5$, in which uranium can be tetra-
164 or pentavalent and corresponding cell parameters are greater than those of stoichiometric CaUO_4
165 (Loopstra and Rietveld 1969; Prodan and Boswell 1986; Takachashi et al. 1993). However,
166 presence of significant oxygen vacancies in vorlanite can be excluded based on site occupation
167 refinements performed by us. Test refinements (not shown) converged at an O population of
168 0.98(4). Thus, in subsequent refinements the value was fixed at 1 (Tables 2-4). If the structures of
169 trigonal uranate and vorlanite are compared, it becomes obvious that disordered cubic vorlanite has
170 larger volume 77.92 \AA^3 (half unit cell volume for comparison with the trigonal uranate) and lower
171 density 7.29 g/cm^3 compared to the ordered uranate: $V = 76.26 \text{ \AA}^3$ and $\rho = 7.45 \text{ g/cm}^3$ of same
172 composition (Galuskin et al. 2011). The cell parameter and the unit volume $V = 2 \times 77.20(2) \text{ \AA}^3$ of
173 dark-grey vorlanite from Jabel Harmun are significantly lower (increased density of 7.36 g/cm^3)
174 than those of Caucasian vorlanite.

175 Systematic survey of the color of vorlanite from different rocks of the Hatrurin formation
176 from the Jabel Harmun (the Judean Desert) and the Hatrurim Basin (the Negev Desert) showed, that
177 in larnite and spurrite rock all vorlanite crystals are dark-gray in transmitted light (Fig. 3A, B). In
178 larnite rocks vorlanite is usually presented by individual crystals (Fig. 1A). In spurrite rocks
179 micron-sized vorlanite crystals form spot-like aggregates (Fig. 3A, B) often overgrowing
180 pseudomorphs of uranium-bearing lakargiite after zircon (Fig. 3C). Lakargiite with UO₃ content up
181 to 20 wt. % was detected in rocks of the Hatrurim formation for the first time. Lakargiite CaZrO_3 ,
182 first discovered in altered xenoliths of the Upper Chegem caldera, was also associated with
183 vorlanite (Galuskin et al. 2008, 2009, 2011).

184 In only one case, in small veins of paralavas of the Gurim anticline (the Negev Desert) rare
185 vorlanite crystals were found (Fig. 3), which appear red-brown in transmitted light. The main
186 minerals of Gurim paralavas are coarse-grained schorlomite, rankinite, melilite, parawollastonite,
187 kalsilite, fluorapatite-fluorellestadite, Fe^{3+} - analog of dorrite, barioferrite and ferric spinel
188 represented by the solid solution magnesioferrite-trevorite-franklinite-cuprospinel. Divalent iron is
189 essentially absent in the composition of ferrites and garnets of paralavas indicating strongly
190 oxidizing conditions. The presence of dorrite-like minerals and also previous investigations of melt
191 inclusions suggest that these paralavas formed above 1100-1200°C (Sharygin et al. 2006a, b).

192 Temperature and pressure, at which “protovorlanite” formed in the different
193 pyrometamorphic rocks, were similar and correspond to conditions of the sanidinite facies.
194 “Protovorlanite”, an orthorhombic uranate CaUO_4 , is stable below 1100°C (Pialoux and Touzelin
195 1998). In small xenoliths of the Caucasus rocks and paralava bodies of the Gurim anticline
196 “protovorlanite” formed in open systems characterized by high oxygen fugacity, i.e. all uranium
197 was hexavalent $6+$. In pyrometamorphic rocks of the Hatrurim formation, characterized by a dense
198 fine-grained larnite and spurrite matrix, crystallization of “protovorlanite” proceeded under the
199 conditions of limited oxygen fugacity, i.e. U^{4+} may enter the structure of “protovorlanite”. In the
200 course of polymorphic transformation “protovorlanite – vorlanite” as a result of radioactive decay,
201 vorlanite inherited insignificant U^{4+} , which may be responsible for its dark-gray color with greenish
202 hue in transmitted light.

203

204 **ACKNOWLEDGMENTS**

205 We thank Robert Finch, Stuart Mills and associate editor Peter C. Burns for constructive and
206 helpful reviews. The work was partly supported by the National Science Centre (NCN) of Poland,
207 grant no. DEC 2012/05/B/ST10/00514.

208

209 **REFERENCES**

210 Burg, A., Starinsky, A., Bartov, Y., and Kolodny, Y. (1991) Geology of the Hatrurim Formation

- 211 (“Mottled zone”) in the Hatrurim Basin. *Israel Journal of Earth Sciences*, 40, 225-234.
- 212 Burg, A., Kolodny, Y., and Lyakhovsky, V. (1999) Hatrurim-2000: The “Mottled Zone”
213 revisited, forty years later. *Israel Journal of Earth Sciences*, 48, 209–223.
- 214 Galuskin, E.V., Gazeev, V.M., Armbruster, T., Zadov, A.E., Galuskina, I.O., Pertsev, N.N.,
215 Dzierżanowski, P., Kadiyski, M., Gurbanov, A.G., Wrzalik, R., and Winiarski, A. (2008)
216 Lakargiite, CaZrO₃: a new mineral of the perovskite group from the North Caucasus,
217 Kabardino-Balkaria, Russia. *American Mineralogist*, 93, 1903–1910.
- 218 Galuskin, E.V., Gazeev, V.M., Lazic, B., Armbruster, T., Galuskina I.O., Zadov, A.E., Pertsev,
219 N.N., Wrzalik, R., Dzierżanowski, P., Gurbanov, A.G., and Bzowska, G. (2009) Chegemite,
220 Ca₇(SiO₄)₃(OH)₂ – a new calcium mineral of the humite-group from the Northern Caucasus,
221 Kabardino-Balkaria, Russia. *European Journal of Mineralogy*, 21, 1045-1059.
- 222 Galuskin, E.V., Armbruster, T., Galuskina, I.O., Lazic, B., Winiarski, A., Gazeev, V.M.,
223 Dzierżanowski, P., Zadov, A.E., Pertsev, N.N., Wrzalik, R., Gurbanov, A.G., and Janeczek, J.
224 (2011) Vorlanite (CaU⁶⁺)O₄ – a new mineral from the Upper Chegem caldera, Kabardino-
225 Balkaria, Northern Caucasus, Russia. *American Mineralogist*, 96, 188-196.
- 226 Galuskin, E.V., Galuskina, I.O., Dubrovinsky, L.S., and Janeczek, J. (2012) Thermally induced
227 transformation of vorlanite to “protovorlanite”: Restoration of cation ordering in self-
228 irradiated CaUO₄. *American Mineralogist*, 97, 1002–1004.
- 229 Galuskin, E.V., Galuskina, I.O., Kusz, J., Armbruster, T., Bailau, R., Dulski, M., Gazeev, V.M.,
230 Pertsev, N.N., Zadov, A.E., and Dzierżanowski, P. (2013a) Kyuygenite, IMA 2012-046.
231 CNMNC Newsletter No. 15, February 2013, page 2; *Mineralogical Magazine*, 77, 1-12.
- 232 Galuskin, E.V., Gfeller, F., Armbruster, T., Galuskina, I.O., Vapnik, Ye., Murashko, M., Włodyka, R.,
233 and Dzierżanowski, P. (2013b) Nabimusaite, IMA2011-112. CNMNC Newsletter No. 15,
234 February 2013, page 5; *Mineralogical Magazine*, 77, 1-12.
- 235 Galuskina, I.O., Vapnik, Ye., Lazic, B., Armbruster, T., Murashko, M., and Galuskin, E.V. (2013)
236 Harmunite, IMA2011-112. CNMNC Newsletter No. 15, February 2013, page 2;
237 *Mineralogical Magazine*, 77, 1-12.

- 238 Gross, S. (1977) The mineralogy of the Hatrurim Formation, Israel. Geological Survey of
239 Israel Bulletin, 70, 1-80.
- 240 Janeczek, J. and Ewing, R.C. (1992) Structural formula of uraninite. Journal of Nuclear Materials,
241 190, 128–132.
- 242 Kolodny, Y. and Gross, S. (1974) Thermal metamorphism by combustion of organic matter:
243 isotopic and petrological evidence. Journal of Geology, 82, 489–506.
- 244 Liegeois-Duyckaerts, M. (1977) Infrared and Raman spectrum of CaUO_4 : New data and
245 interpretation. Spectrochimica Acta Part A; Molecular Spectroscopy, 6-7, 709–713.
- 246 Loopstra, B.O. and Rietveld, H.M. (1969) The structure of some alkaline-earth metal uranates. Acta
247 Crystallographica, B25, 787–791.
- 248 Othmane, G., Allard, T., Menguy, N., Morin, G., Esteve, I., Fayek, M., and Calas, G. (2013)
249 Evidence for nanocrystals of vorlanite, a rare uranate mineral, in the Nopal I low-
250 temperature uranium deposit (Sierra Peña Blanca, Mexico. American Mineralogist, 98, 518-
251 521.
- 252 Pialoux, A. and Touzelin, B. (1998) Étude du système U-Ca-O par diffractométrie de rayons X à
253 haute température. Journal of Nuclear Materials, 255, 14–25.
- 254 Picard, L. (1931) Geological Research in the Judean Desert. Goldberg Press, Jerusalem.
255 108.
- 256 Plant, J.A., Simpson, P.R., Smith, B., and Windley, B. (1999) Uranium ore deposits – products of
257 the radioactive Earth. In Uranium: Mineralogy, Geochemistry and the Environment (Eds.
258 Burns, P.C. and Finch, R.). Reviews in Mineralogy, 38, 255-319.
- 259 Prodan, A. and Boswell, F. W. (1986) The defect structure of reduced CaUO_4 . Acta
260 Crystallographica, B42, 141-146.
- 261 Sharygin, V.V., Vapnik, Ye., Sokol, E.V., Kamenetsky, V.S., and Shagam, R. (2006a) Melt
262 inclusions in minerals of schorlomite-rich veins of the Hatrurim Basin, Israel: composition
263 and homogenization temperatures. In: ACROFI I, Program with Abstracts (Ed. by N. Pei &
264 L. Zhaolin), pp. 189–192. Nanjing, China, 26-28 May 2006.

- 265 Sharygin, V.V., Vapnik, Ye., Sokol, E.V., and Shagam, R. (2006b) Kalsilite-schorlomite-melilite
266 rocks of Hatrurim Formation – products of pyrogenic alkaline melt crystallization: data on
267 mineralogy and melt inclusions. Abstracts of All Russian seminar “Geochemistry of
268 magmatic rocks” [school “Alkaline magmatism of Earth”] (in Russian)
269 <http://geo.web.ru/conf/alkaline/2006/index22.html>.
- 270 Sharygin, V.V., Lazic, B., Armbruster, T.M., Murashko, M.N., Wirth, R., Galuskina, I.O.,
271 Galuskin, E.V., Vapnik, Ye., Britvin, S.N., and Logvinova A.M. (2013) Shulamitite
272 $\text{Ca}_3\text{TiFe}^{3+}\text{AlO}_8$ - a new perovskite-related mineral from Hatrurim Basin, Israel. European
273 Journal of Mineralogy, 25, 97-111.
- 274 Sheldrick, G.M. (2008) A short history of SHELX. Acta Crystallographica, A64, 112–122.
- 275 Sokol, E.V., Novikov, I.S., Vapnik, Ye., and Sharygin, V.V. (2007) Gas fire from mud volcanoes
276 as a trigger for the appearance of high-temperature pyrometamorphic rocks of the Hatrurim
277 Formation (Dead Sea area). Doklady Earth Sciences, 413A, 474–480 (in Russian).
- 278 Sokol, E., Novikov, I., Zateeva, S., Vapnik, Ye, Shagam, R., and Kozmenko, O. (2010) Combustion
279 metamorphism in the Nabi Musa dome: new implications for a mud volcanic origin of the
280 Mottled Zone, Dead Sea area. Basin Research, 22, 414–438.
- 281 Tagawa, H., Fujino, T., and Tateno, J. (1997) Formation of strontium uranates. Bulletin Chemical
282 Society of Japan, 50, 2940-2944.
- 283 Takahashi, K., Fujino, T., and Morsse, L.R. (1993) Crystal chemical and thermodynamic study on
284 CaUO_{4-x} , $(\text{Ca}_{0.5}\text{Sr}_{0.5})\text{UO}_{4-x}$, and $\alpha\text{-SrUO}_{4-x}$ ($x = 0 \sim 0.5$). Journal of Solid State Chemistry,
285 105, 234-246.
- 286 Terra, O., Audubert, F., Dacheux, N., Guy, C., and Podor, R. (2007) Synthesis and characterization
287 of uranium-bearing britholites. Journal Nuclear Materials, 366, 70-86.
- 288 Vapnik, Y., Sharygin, V.V., Sokol, E.V., and Shagam R. (2007) Paralavas in a combustion
289 metamorphic complex: Hatrurim Basin, Israel. Reviews in Engineering Geology, 18, 1-21.
- 290 Wyckoff, R. W. G. (1963) Crystal Structures, 1, 239-444.
- 291

292 Figures

293

294 Fig. 1. A – Poikilitic crystals of vorlanite in larnite-brownmillerite-ye'elimite-mayenite rock.

295 Magnified crystal in Fig. 1B and C is framed. Oldhamite, CaS, phosphoresces under the electron

296 beam. Fragments of the second crystal of vorlanite at the bottom on the right of the BSE image

297 were used for single X-ray diffraction study; B, C – vorlanite crystal used in Raman spectroscopic

298 experiment: B – BSE image, arrow points to a crater burned by laser, C – transmitted light picture

299 with switched on condenser lens; around the crater vorlanite transformed to yellow rhombohedral

300 uranate; inset at the bottom right: red grain of vorlanite from Caucasus (30×20×6 μm),

301 distinguished in color from dark-grey Jabel Harmun vorlanite.

302 Vor - vorlanite, Ye - ye'elimite, Old - oldhamite, Lar - larnite, Ell - fluorellestadite, Brm -

303 brownmillerite.

304

305 Fig. 2. Raman spectra of vorlanite: 1 – Jabel Harmun locality, 2 – Caucasus type locality and 1*, 2*

306 - products of its thermal transformation, respectively.

307

308 Fig. 3. A, B – vorlanite in spurrite rock (A – BSE, B - transmitted light with switched on condenser

309 lens); C – vorlanite crystals on U-bearing lakargiite pseudomorphs after zircon; D - Crystal of red-

310 brown vorlanite overgrowing perovskite, sample from paralava of the Gurim anticline, the Hatrurim

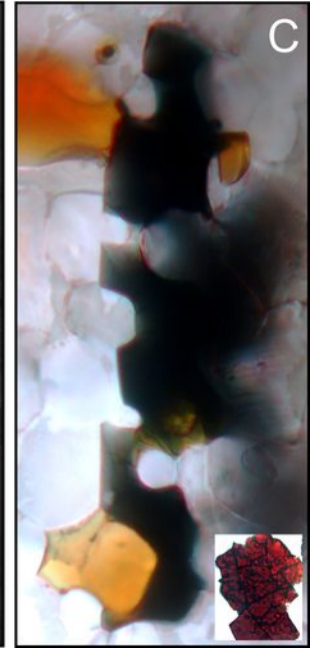
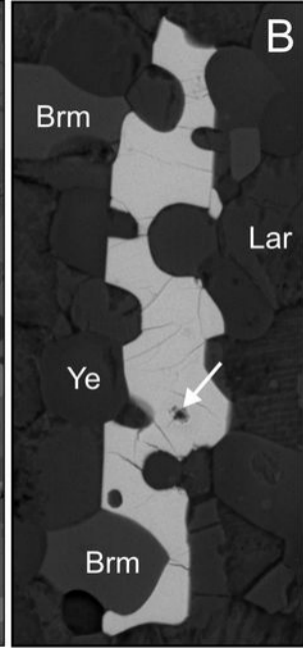
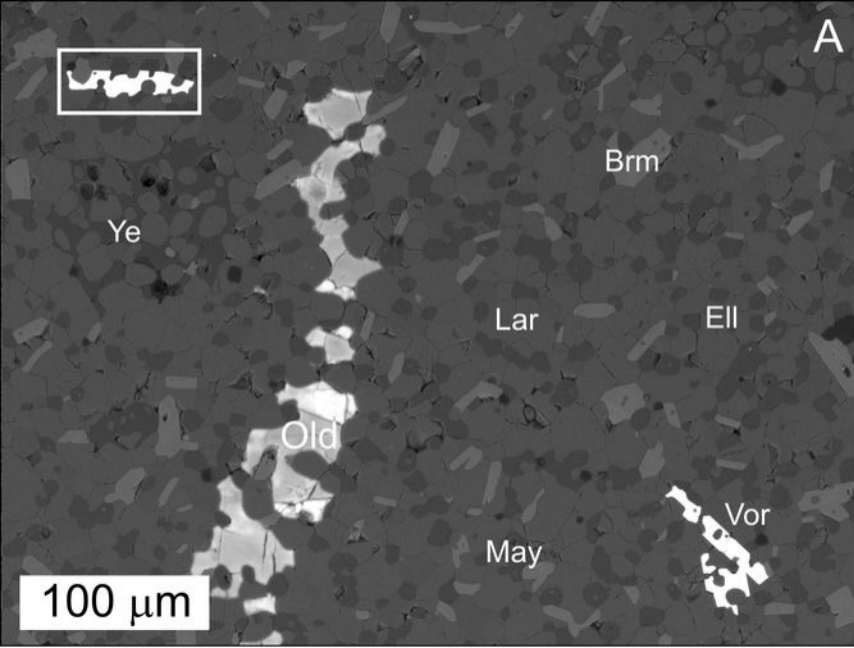
311 Basin, the Negev Desert. A – BSE, framed area is magnified in Fig. 3E; E – transmitted light with

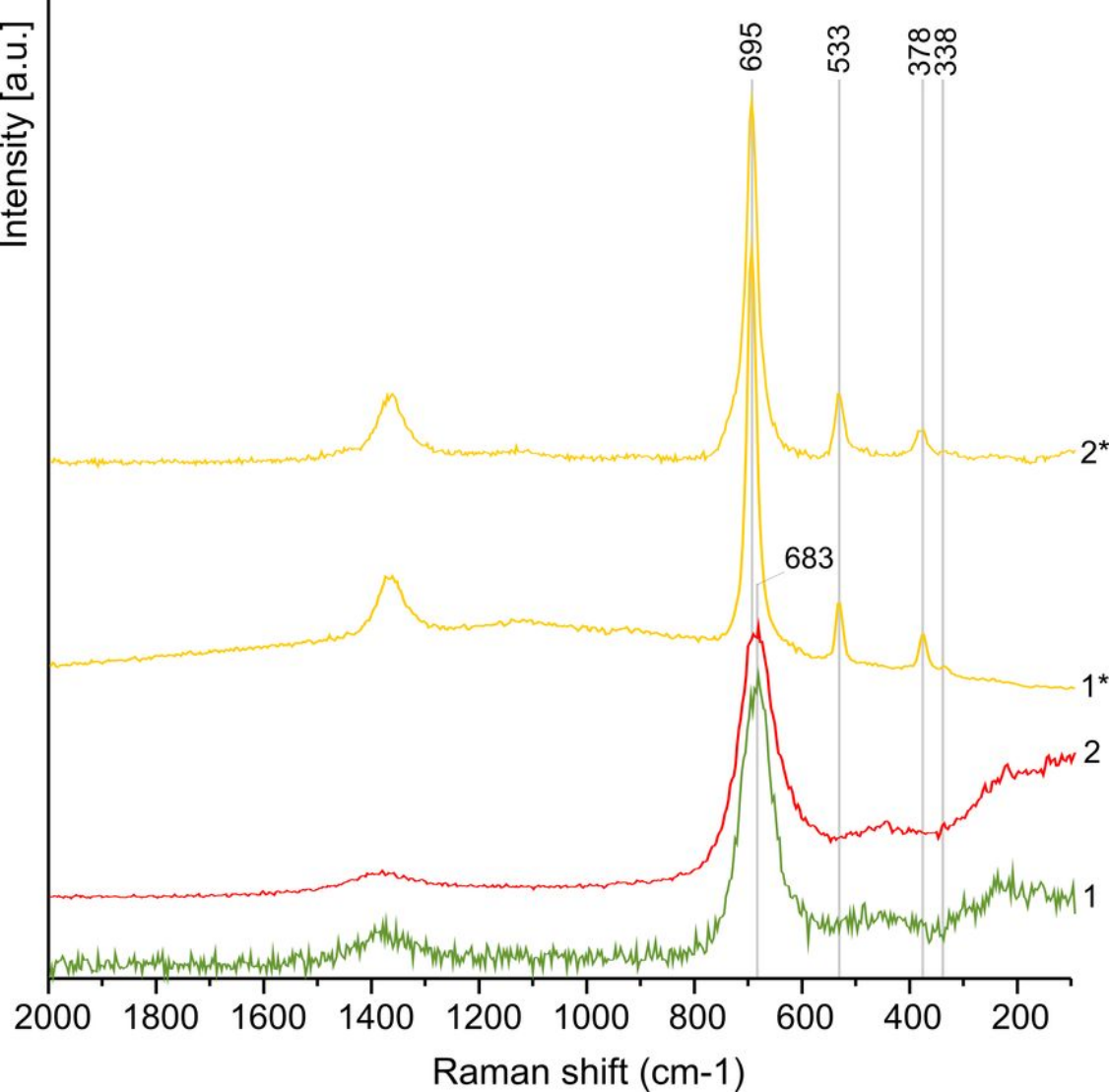
312 switched on condenser lens.

313 Vor - vorlanite, Rnk - rankinite, Wol - wollastonite, Mel - melilite, Prv - perovskite, Ell -

314 fluorellestadite-fluorapatite series, Dor - Fe³⁺-analog of dorrite.

315





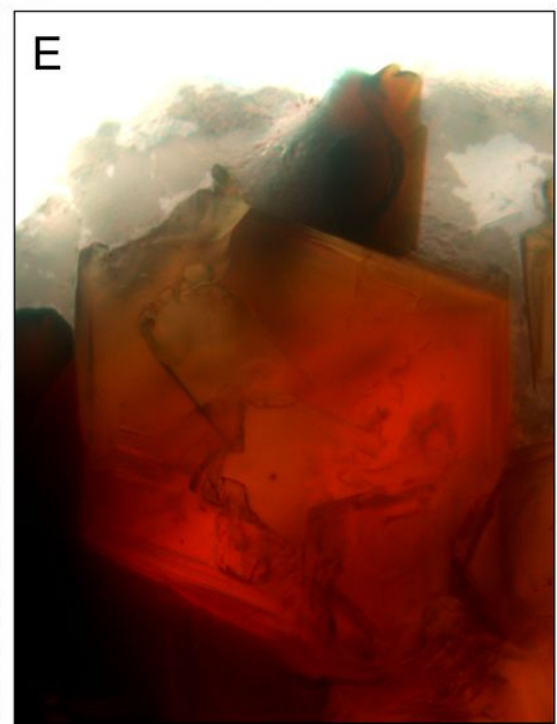
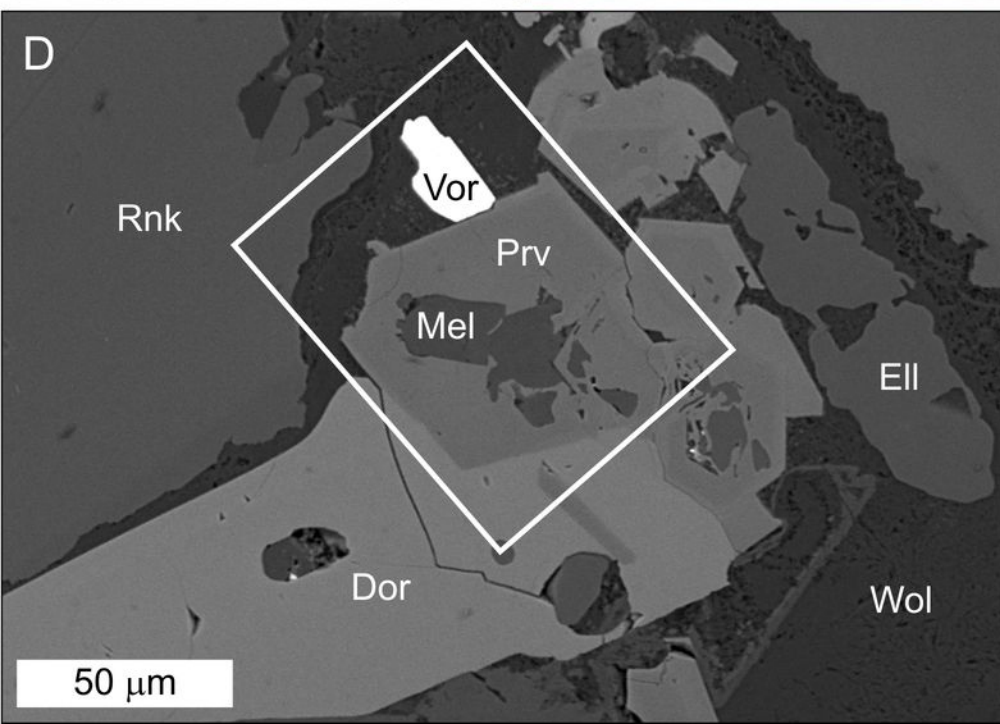
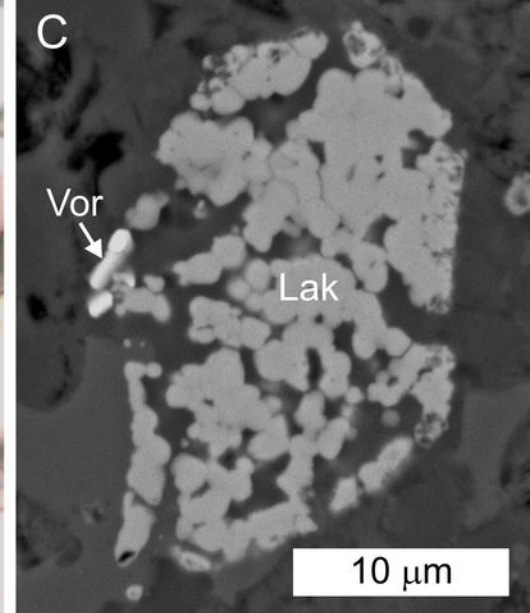
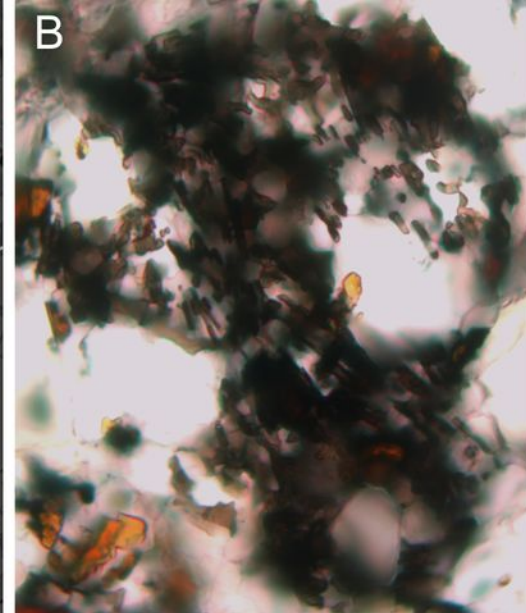
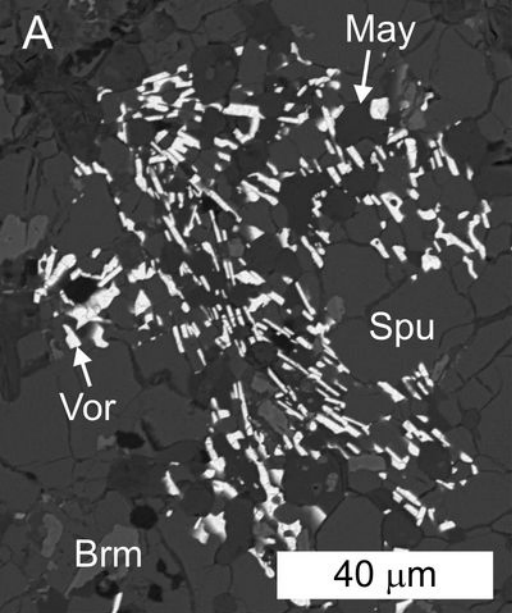


Table 1. Chemical composition of vorlanite from Jabel Harmun locality.

wt%	mean 13	s.d.	range
UO ₃	83.79	0.37	83.17-84.40
CaO	16.77	0.04	16.68-16.81
Fe ₂ O ₃	0.04	0.04	0-0.14
Total	100.56		
calculated on 2 cations			
U ⁶⁺	0.989		
Ca	1.009		
Fe ³⁺	0.002		

Table 2. Data collection and structure refinement details for vorlanite

Temperature	296(2) K
Theta range for data collection	6.59 for 41.48°
Index ranges	$-10 \leq h \leq 9, -9 \leq k \leq 9, -10 \leq l \leq 9$
Reflections collected	1631
Independent reflections	46 [$R_{\text{(int)}} = 0.0575; R_{\sigma} = 0.0114$]
Crystal size	$0.008 \times 0.010 \times 0.020$ mm
Crystal system	cubic
Space group	$Fm\bar{3}m$
Unit cell dimensions	$a = 5.3647(9) \text{ \AA} \alpha = 90^{\circ}$
V	$154.40(4) \text{ \AA}^3$
Z	2
D_{calc}	7.359 g cm^{-3}
Goodness-of-fit on F^2	1.212
Final R indices	46 data; $I > 4\sigma(I)$, $R1 = 0.0088$ all data $R1 = 0.0088$, $wR2 = 0.0174$
Largest diff. peak and hole	0.260 and -0.358 e\AA^{-3}

Table 3. Atomic coordinates and equivalent isotropic atomic displacement parameters (\AA^2) for vorlanite

Atom	x/a	y/b	z/c	sof	U_{eq}
U	0	0.5	0	0.5	0.01848(9)
Ca	0	0.5	0	0.5	0.01848(9)
O	0.25	0.25	0.25	1	0.0614(15)

isotropic displacement parameters for all sites because $U_{11}=U_{22}=U_{33}$ and $U_{12}=U_{13}=U_{23}=0$

Table 4. Bond lengths (Å) and angles (°) for vorlanite

Atoms			Bond length (Å)	mult.
U1/Ca1	O1		2.3230(4)	x 8
U1/Ca1	U1/Ca1		3.7934(6)	x 4
Atoms			Angle (°)	mult.
O1	U1/Ca1	O1	180.0	x 4
O1	U1/Ca1	O1	109.47	x 12
O1	U1/Ca1	O1	70.53	x 12